Discrete Constitutive Equations in A-χ Geometric Eddy-Current Formulation

Ruben Specogna and Francesco Trevisan

Dipartimento di Ingegneria Elettrica, Gestionale e Meccanica Università di Udine, 33100 Udine, Italy

Using a geometric formulation for eddy currents, we present a geometric approach to constructing approximations of the discrete magnetic and Ohm's constitutive matrices. In the case of Ohm's matrix, we also show how to make it symmetric. We compared the impact on the solution of the proposed Ohm's matrices, and an iterative technique to obtain a consistent right-hand-side term in the final system is described.

***Index Terms*—Cell complexes, cell method, constitutive matrices, eddy currents.**

I. INTRODUCTION

THE role of geometry in the discretization of continuous field equations and of constitutive equations [6], [7], [20], [21], reveals to be very important in the derivation of the algebraic systems of equations with respect to a finite-element mesh. We will start from an algebraic formulation, named A-χ and proposed in [24], to solving eddy currents in linear media. To underline the geometric structure behind this formulation, we will collocate it within the so-called Tonti's diagram [19].

We will also focus on discrete constitutive equations, proposing an efficient way to compute geometrically the discrete magnetic constitutive matrix and different ways to compute Ohm's discrete constitutive matrix. We will show how a symmetric Ohm's matrix can be obtained. The interest in this kind of research is documented also in [9], [17], and [10] for the case of electric constitutive matrix in wave-propagation problems.

As a test problem we will consider a benchmark, proposed and developed by the University of Perugia in the framework of an Italian research project on nondestructive testing (named MADEND project [8]). We will compare the numerical results obtained solving the reference problem, with those from a commercial finite-element code, when different Ohm's matrices are used. Finally, convergence and accuracy between the proposed approach and finite elements will be examined numerically with respect to the same mesh.

II. PRELIMINARIES

The domain of interest D consists of a conducting region D_c, where a conductor is present (containing a defect), of a source region D_s, where a coil with a specified geometry and with impressed current is located, and an air region D_a, which is the complement of D_c and D_s in D. The field quantities of interest in an eddy-current problem can be represented with differential p-forms [4], [11], such as the 1-form u of the electric field, the 2-form b of the induction field, the twisted 1-form h of the magnetic field and the twisted 2-form j of the current density. We introduce in D a pair of interlocked cell complexes: The primal $\mathcal{K}$ and its barycentric dual $\tilde{\mathcal{K}}$, [5, p. 136], [22]. The p-cells of $\mathcal{K} = \{\mathcal{N}, \mathcal{E}, \mathcal{F}, \mathcal{V}\}$ are simplices, such as nodes $n \in \mathcal{N}$, edges $e \in \mathcal{E}$, faces (triangles) $f \in \mathcal{F}$, and volumes (tetrahedra) $v \in \mathcal{V}$ all endowed with *inner* orientation. The p-cells of $\tilde{\mathcal{K}} = \{\tilde{\mathcal{V}}, \tilde{\mathcal{F}}, \tilde{\mathcal{E}}, \tilde{\mathcal{N}}\}$ are all endowed with *outer* orientation and are obtained from $\mathcal{K}$ according to the barycentric subdivision. The pair $\{\mathcal{K}, \tilde{\mathcal{K}}\}$ forms the mesh $\mathcal{M}$. The mutual interconnections of the primal cell complex $\mathcal{K}$ are described by the incidence matrices: $\mathbf{G}$ between edges e and nodes n, $\mathbf{C}$ between faces f and edges e, and $\mathbf{D}$ between volumes v and faces f. The matrices $\tilde{\mathbf{G}} = \mathbf{D}^T$, $\tilde{\mathbf{C}} = \mathbf{C}^T$, and $\tilde{\mathbf{D}} = -\mathbf{G}^T$[1] describe the mutual interconnections of $\tilde{\mathcal{K}}$.

We use the *de Rham map* $r_{\mathcal{M}}$, [7], which sends a p-differential form to the corresponding array of degrees of freedom (DoF) relative to the corresponding p-cells of mesh $\mathcal{M}$. Therefore, we have that $r_{\mathcal{M}} b = \mathbf{\Phi}$ is the array of fluxes on primal faces f, $r_{\mathcal{M}} u = \mathbf{U}$ is the array of electromotive force on primal edges e, $r_{\mathcal{M}} h = \mathbf{F}$ is the array of magnetomotive force (MMF) on dual edges $\tilde{e}$ and $r_{\mathcal{M}} j = \mathbf{I}$ is the array of currents on dual faces $\tilde{f}$. The DoF arrays are regarded here as functions of a time instant. Physical laws governing an eddy-current problem can now be written directly in an algebraic way as follows:

$$\begin{aligned} &\mathbf{D\Phi} = \mathbf{0} \text{ (Gauss law)}, && \tilde{\mathbf{C}}\mathbf{F} = \mathbf{I} \text{ (Ampere law)} \\ &\mathbf{CU} = -d_t\mathbf{\Phi} \text{ (Faraday law)}, && \tilde{\mathbf{D}}\mathbf{I} = \mathbf{0} \text{ (continuity law)}. \end{aligned} \tag{1}$$

Physical laws written in this way are metric independent and they are *exact* independently of the size of the mesh $\mathcal{M}$. On the contrary, constitutive laws are *pointwise* relations between fields and, to discretize them on a mesh, we need to compute discrete approximated operators linking the DoF arrays such as

$$\mathbf{F} = \boldsymbol{\nu}\mathbf{\Phi}, \quad \mathbf{I} = \boldsymbol{\sigma}\mathbf{U} \tag{2}$$

where $\boldsymbol{\nu}$ and $\boldsymbol{\sigma}$ are some square mesh- and medium-dependent matrices that require *metric* notions, *material* properties, and some hypothesis on the *fields* in order to be computed. The discrete eddy-current problem (DEC), for the mesh $\mathcal{M}$, consists of computing the arrays $\mathbf{\Phi}$, $\mathbf{U}$, $\mathbf{F}$, and $\mathbf{I}$, such that (1) and (2) *hold*

[1]The minus sign comes from the assumption that n is oriented as a sink, whereas the boundary of $\tilde{v}$ is oriented by the outer normal.

Digital Object Identifier 10.1109/TMAG.2005.844841

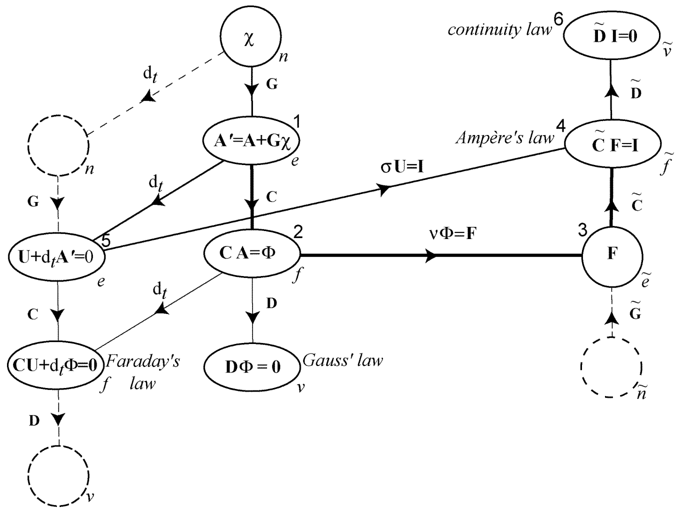

Fig. 1. Tonti's diagram for eddy currents.

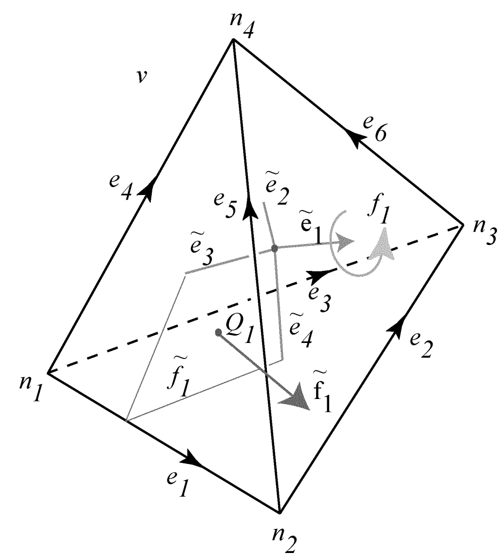

Fig. 2. Geometric elements of a mesh $\mathcal{M}$ reduced to a single tetrahedron v.

simultaneously, when sources are assigned in D_s as impressed currents $\mathbf{I} = \mathbf{I}_s$ together with initial and boundary conditions.

III. Geometric Formulation for Eddy Currents

A possible way to solve the DEC problem is to introduce a pair of potentials a and χ such that $r_{\mathcal{M}}\chi = \boldsymbol{\chi}$ is the array of gauge function values on primal nodes n of D_c and $r_{\mathcal{M}}a = \mathbf{A}$ is the array of circulations of magnetic vector potential on primal edges e of D, respectively. Considering the array $\mathbf{A}' = \mathbf{A} + \mathbf{G}\boldsymbol{\chi}$ associated with primal edges e, Gauss's and Faraday's laws in (1) are satisfied identically[2] when we write respectively

$$\boldsymbol{\Phi} = \mathbf{C}\mathbf{A}, \quad \mathbf{U} = -d_t\mathbf{A}'. \tag{3}$$

Combining (1), (3), and (2), we obtain, in the frequency domain $(d_t \rightarrow i\omega)$, the following equations:

$$\begin{array}{ll} \tilde{\mathbf{C}}\boldsymbol{\nu}\mathbf{C}\mathbf{A} = \mathbf{I} & \forall e \in D_a \cup D_s, \\ (\tilde{\mathbf{C}}\boldsymbol{\nu}\mathbf{C} + i\omega\boldsymbol{\sigma})\mathbf{A} + i\omega\boldsymbol{\sigma}\mathbf{G}\boldsymbol{\chi} = 0 & \forall e \in D_c, \\ i\omega\tilde{\mathbf{D}}\boldsymbol{\sigma}\mathbf{A} + i\omega\tilde{\mathbf{D}}\boldsymbol{\sigma}\mathbf{G}\boldsymbol{\chi} = 0 & \forall n \in D_c \end{array} \tag{4}$$

where the DoF arrays are now complex variables. This is the so-called A-χ geometric formulation. From it, χ being arbitrary, the so-called A formulation [14] may be obtained as a particular case, by eliminating χ and the last set of equations in (4); the convergence of A formulation depends strongly on the choice of the preconditioner as shown in [15], [16], and an appropriate state of the art preconditioner may exhibit a superior convergence behavior in comparison with A-χ formulation.

A synthetic tool that gives relevance to the geometric aspects and allows to derive the above equations is the Tonti's diagram (for a comprehensive description, see [19]). Here, we derive it at discrete level for our DEC problem, Fig. 1. On the left side of the diagram, two vertical pillars are drawn, where each DoF array[3] is associated with the corresponding geometric element of the primal cell complex (nodes to volumes, from top to bottom). On the right side of the diagram, only one of the two vertical pillars needs to be drawn for the case of eddy currents, where each DoF array[4] is associated with the corresponding geometric element of the dual complex (nodes to volumes, from bottom to top). The dashed circles represent categories not used in the specific problem.[5] The discrete constitutive equations (2) are represented as horizontal links from left to right. Along a vertical pillar, we move from the variables on one level to the variables on the successive level (for example, from $\mathbf{A}'$ on edges e to $\boldsymbol{\Phi}$ on faces f) of the primal or of the dual complex, using the incidence matrices. This process[6] allows us to form, at each level, algebraic relations between variables such as the physical laws in discrete form (1). We can derive the first set of equations in (4), following the path 1-2-3-4 in the diagram (see Fig. 1). The second set of equations in (4) comes from the path 1-2-3-4 together with the path 1-5-4. Finally, the last set of equations in (4) corresponds to the path 1-5-4-6.

IV. Discrete Constitutive Equations

Without losing generality, we may limit the primal mesh to a single tetrahedron v under the assumption of homogeneity of the medium in it so that the reluctivity ν or the conductivity σ are constants. All results derived in this particular case can easily be extended to a mesh consisting of tetrahedra, where each element may model different media. By linearity, the global matrices $\boldsymbol{\nu}$ or $\boldsymbol{\sigma}$ can be assembled from the contributions of the single elements. Recalling a result demonstrated in [23], we will derive the elements of a matrix $\boldsymbol{\nu}$ in a very efficient way. We refer to Fig. 2, where a primal edge is inner oriented from the lower label to the higher label of its bounding nodes and a face is inner-oriented in such a way that its orientation matches the orientations

[2]Mesh $\mathcal{M}$ is formed by cell complexes and, hence, the identities $\mathbf{DC} = 0$, $\mathbf{CG} = 0$ hold.

[3]These DoF arrays are called *configuration* variables.

[4]These DoF arrays are called *source* variables.

[5]For example the top left empty circle is reserved to the electric scalar potential V, not used in this formulation; its relation with χ is $V = d_t\chi$, and for this χ is also referred to as time-integrated scalar potential.

[6]More formally, this is the *co-boundary* process.

of two of its bounding edges. We inner-orient a cell v according to *Möbius rule*.[7]

We express the induction field B in v (denoted in roman type) in terms of Whitney face elements and using Gauss' law (1), we obtain

$$\mathrm{B} = \frac{1}{3\mathrm{vol}(v)}(\Phi_1 \mathrm{e}_4 - \Phi_2 \mathrm{e}_5 + \Phi_3 \mathrm{e}_6) \tag{5}$$

where Φ_i, with $i = 1, \ldots, 3$ is the flux associated with face f_i and e_k, with $k = 4, \ldots, 6$, is the vector associated with edge e_k. Field $\mathrm{H} = \nu\mathrm{B}$ is uniform in v, and MMF F_i along a dual edge $\tilde{e}_i$ becomes

$$F_i = \mathrm{H} \cdot \tilde{\mathrm{e}}_i, \quad i = 1, \ldots, 4 \tag{6}$$

where $\tilde{\mathrm{e}}_i$ is the edge vector associated with $\tilde{e}_i$. Then the ith row $\boldsymbol{\nu}_i$, with $i = 1, \ldots, 4$, of a possible constitutive matrix $\boldsymbol{\nu}$ for the considered mesh is

$$\boldsymbol{\nu}_i = \nu(\tilde{\mathrm{e}}_i \cdot \mathrm{e}_4, \quad -\tilde{\mathrm{e}}_i \cdot \mathrm{e}_5, \quad \tilde{\mathrm{e}}_i \cdot \mathrm{e}_6, \quad 0). \tag{7}$$

The constitutive matrix $\boldsymbol{\nu}$ derived this way, is nonsymmetric and singular, but what really matters is that the matrix $\tilde{\mathbf{C}}\boldsymbol{\nu}\mathbf{C}$ is symmetric positive semidefinite [23], and that it coincides with the matrix one can obtain using finite elements based on Whitney edge elements [18].

Now we will deduce the discrete Ohm's constitutive matrix $\boldsymbol{\sigma}$. We approximate the electric field vector E in each cell v by means of an *affine* field. A simple way to generate in v an affine E, from the six voltages U_j on primal edges e_j, is

$$\mathrm{E}(P) = \sum_{j=1}^{6} \mathrm{w}_j(P) U_j \tag{8}$$

where $\mathrm{w}_j(P) = w_{n_h}\nabla w_{n_k} - w_{n_k}\nabla w_{n_h}$ is the jth Whitney vector function of degree 1 associated with edge e_j (of nodes n_h, n_k) and w_{n_h} is the affine nodal function for node n_h, P is any point in v. The current density vector $\mathrm{J}(P) = \sigma\mathrm{E}(P)$ is affine in v, and the electric current I_i across a dual face $\tilde{f}_i$ (with associated area vector $\tilde{\mathrm{f}}_i$, see Fig. 2) becomes

$$I_i = \int_{\tilde{f}_i} \mathrm{J} \cdot d\mathrm{s} = \mathrm{J}(Q_i) \cdot \tilde{\mathrm{f}}_i, \quad i = 1, \ldots, 6 \tag{9}$$

where $\mathrm{J}(Q_i)$ is the current density evaluated at the barycentre Q_i of the dual face $\tilde{f}_i$. Then the element $\sigma_{i,j}$ of a constitutive matrix $\boldsymbol{\sigma}$ for the considered mesh is

$$\sigma_{i,j} = \sigma\tilde{\mathrm{f}}_i \cdot \mathrm{w}_j(Q_i), \quad i, j = 1, \ldots, 6. \tag{10}$$

The matrix $\boldsymbol{\sigma}$ obtained this way is nonsymmetric but, it is easy to prove in a way similar to that shown in [23], that the matrix $\tilde{\mathbf{D}}\boldsymbol{\sigma}\mathbf{G}$ is still symmetric and positive semidefinite, and it coincides with that from nodal finite elements based on Whitney nodal functions.

This constitutive matrix $\boldsymbol{\sigma}$ makes the global system matrix in (4) nonsymmetric. We will now suggest two approaches to derive a symmetric Ohm's matrix.

A first approach considers the dissipated power P in the conductor region. We focus on a tetrahedron $v \in D_c$, and we write $P = \int_v \mathrm{E} \cdot \mathrm{J}\, dv$; by substituting in it (8) for E and assuming $\mathrm{J} = \mathrm{J}^u$ uniform in v, we have

$$P \simeq \sum_{j=1}^{6} U_j \mathrm{J}^u \cdot \int_v \mathrm{w}_j dv = \sum_{j=1}^{6} U_j \mathrm{J}^u \cdot \mathrm{w}_j(\tilde{n}) V \tag{11}$$

where V is the volume of v and $\tilde{n}$ is its barycentre.[8] Using the geometric interpretation of ∇w_{n_h} shown in [23], we can express $\mathrm{w}_j(P)$ as

$$\mathrm{w}_j = \frac{1}{3V}\left(d_{v,h}\mathrm{f}_h w_{n_k} - d_{v,k}\mathrm{f}_k w_{n_h}\right) \tag{12}$$

where f_h and f_k are the area vectors associated with faces f_h and f_k, respectively, $d_{v,h}$, $d_{v,k}$ are incidence numbers between inner orientations of faces f_h, f_k, respectively, and inner orientation of v. For example (see Fig. 2), w_1 attached to edge e_1 with nodes n_1 and n_2, becomes $\mathrm{w}_1 = (\mathrm{f}_1 w_{n_2} - \mathrm{f}_2 w_{n_1})/3V$. Now from a pure geometric property in a tetrahedron with barycentric subdivision, we have that $(1/12)(d_{v,h}\mathrm{f}_h - d_{v,k}\mathrm{f}_k) = \tilde{\mathrm{f}}_j$ holds; for example (refer to Fig. 2), $(1/12)(\mathrm{f}_1 - \mathrm{f}_2) = \tilde{\mathrm{f}}_1$. Being $w_{n_h}(\tilde{n}) = w_{n_k}(\tilde{n}) = 1/4$, (12) becomes

$$\mathrm{w}_j(\tilde{n}) = \frac{1}{V}\tilde{\mathrm{f}}_j \tag{13}$$

and substituting it in (11), we have

$$P \simeq \sum_{j=1}^{6} U_j \mathrm{J}^u \cdot \tilde{\mathrm{f}}_j. \tag{14}$$

Now we may set the uniform current density J^u to $\mathrm{J}^u = \sigma\mathrm{E}(\tilde{n})$, where we use (8) for E. This corresponds to consider in v an average current density vector that coincides with the average of $\mathrm{J}(Q_i)$ in (9), with $i = 1, \ldots, 6$, being $\tilde{n} = \sum_{i=1}^{6} Q_i/6$. Therefore, (14) becomes

$$P \simeq \sum_{j=1}^{6}\sum_{i=1}^{6} U_j \sigma \mathrm{w}_i(\tilde{n}) \cdot \tilde{\mathrm{f}}_j U_i. \tag{15}$$

This way, we derive the elements of a constitutive matrix $\boldsymbol{\sigma}'$ as

$$\sigma'_{i,j} = \sigma \mathrm{w}_i(\tilde{n}) \cdot \tilde{\mathrm{f}}_j \tag{16}$$

where it is straightforward to see that $\sigma'_{i,j} = \sigma'_{j,i}$ and that $\boldsymbol{\sigma}'$ is singular, but $\tilde{\mathbf{D}}\boldsymbol{\sigma}'\mathbf{G} = \tilde{\mathbf{D}}\boldsymbol{\sigma}\mathbf{G}$ still holds. The elements $\sigma'_{i,j}$ in (16) coincide with those of the so-called *mass matrix* of edge elements (see [5]), provided that we compute the integrals using a 1-point quadrature formula, the quadrature point being located in the barycenter of the tetrahedron.

[7]The rule states that the orientations of two adjacent faces counter match on the common edge.

[8]The order of this approximation of P is $\mathcal{O}(s)$, where s is the size of the mesh.

A second approach, purely numerical, consists of decomposing $\boldsymbol{\sigma}$ in (10), in its symmetric (positive definite) and antisymmetric parts as

$$\boldsymbol{\sigma} = \boldsymbol{\sigma}'' + \boldsymbol{\sigma}_a = \frac{1}{2}(\boldsymbol{\sigma} + \boldsymbol{\sigma}^T) + \frac{1}{2}(\boldsymbol{\sigma} - \boldsymbol{\sigma}^T). \quad (17)$$

It follows that $\tilde{\mathbf{D}}\boldsymbol{\sigma}_a\mathbf{G} = 0$ and again $\tilde{\mathbf{D}}\boldsymbol{\sigma}''\mathbf{G} = \tilde{\mathbf{D}}\boldsymbol{\sigma}\mathbf{G}$ holds. It can be also verified that $\|\boldsymbol{\sigma}_a\|/\|\boldsymbol{\sigma}\| < 0.05$. Thus, we consider only $\boldsymbol{\sigma}''$ neglecting $\boldsymbol{\sigma}_a$.

As the mesh size approaches zero, we have that $\tilde{\mathbf{D}}\boldsymbol{\sigma}'$ tends to $\tilde{\mathbf{D}}\boldsymbol{\sigma}$; because $\boldsymbol{\sigma}'$ is structurally symmetric and the norm of $\boldsymbol{\sigma}_a$ is negligible with respect to the norm of $\boldsymbol{\sigma}$, we have also that $\tilde{\mathbf{D}}\boldsymbol{\sigma}''$ will tend to $\tilde{\mathbf{D}}\boldsymbol{\sigma}$.

V. Determination of the Source Currents

We will solve system (4) without gauging, using an iterative solver for nonsymmetric matrices based on the conjugate gradient (from NAG numerical libraries). To assure consistency of the known term in (4), we need

$$\tilde{\mathbf{D}}\mathbf{I}_s = 0 \quad (18)$$

where $\mathbf{I}_s$ is the source current vector in D_s. To compute a solenoidal $\mathbf{I}_s$, different approaches can be used such as those presented in [2], [12]. The approach we follow here starts from a prescribed current density vector J_s in D_s. In our case the coil is circular, and we choose J_s of constant amplitude and tangent to a generic circle laying inside the coil region and coaxial with the coil itself. But in general, a more complicated coil shape can be considered as well. For each tetrahedron $v \in D_s$, we compute the current $\mathrm{J}_s(Q_j) \cdot \tilde{\mathrm{f}}_j$, with $j = 1, \ldots, 6$, with Q_j the barycenter of the portion $\tilde{f}_j$ of a dual face tailored inside the tetrahedron v. Then for each dual face in D_s, we add the total current associated with that dual face. The source currents thus obtained do not comply with (18). Thus, we form a tree and a co-tree based on primal nodes (one-to-one with $\tilde{v}$) and primal edges (one-to-one with $\tilde{f}$) in D_s. Like in basic circuit theory, we keep the currents associated with the edges of the co-tree and we determine the currents associated with the tree edges consistently with (18). We impose this iteratively, without solving any linear system. The algorithm scans all the nodes in D_s and considers the star of edges relative to each node as follows:

1) if the star of edges has only one tree edge, with current not yet computed, then compute the corresponding current consistently with (18) from the other currents relative to that node;
2) remove that node from the list of nodes;
3) restart from 1) until the list of nodes is empty.

Typically the algorithm converges in few iterations.

VI. Numerical Experiments and Results

As reference test problem, we consider the MADEND benchmark 1 (see [13] for a detailed description). It consists of a probe coil (400 turns, 10 mm height, 12 mm inner diameter, 18 mm outer diameter) placed above an aluminum plate (4 mm thick) having 0.5 mm of average lift-off, (Fig. 3 on the left). The volumetric defect $D_d \subset D_c$ is a perfectly insulating cylindrical hole of 1 mm diameter crossing the plate. A reference coil, identical to the probe coil described above, is placed in a region of the metallic plate without defects. The coils are fed with a sinusoidal current of frequency $f = 5000$ Hz and are connected to a bridge to measure the voltage variation ΔU across the two branches of the bridge, for different relative positions $\Delta \mathrm{x}$ between the probe coil and the hole. The voltage variation $\Delta U = f(Z_0, \Delta Z)$ depends on $\Delta Z = Z_d - Z_0$ according to the prescribed nonlinear characteristic function f of the bridge, where Z_0 is the flawless impedance and Z_d is the defected plate impedance.

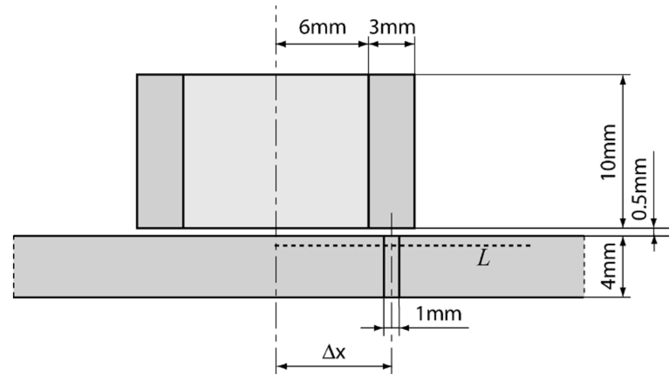

Fig. 3. Benchmark problem geometry.

TABLE I
Results From Different Types of Analysis

Type of analysis	ΔU [Volt]
ΔZ with $\boldsymbol{\sigma}$	3.737e-4
ΔZ with $\boldsymbol{\sigma}'$	3.710e-4
ΔZ with $\boldsymbol{\sigma}''$	3.743e-4
ΔZ with ANSYS	3.777e-4

We studied the impact on ΔZ, of the proposed Ohm's constitutive matrices $\boldsymbol{\sigma}$, $\boldsymbol{\sigma}'$ and $\boldsymbol{\sigma}''$, with respect to the *same* mesh of 30782 tetrahedra. We also compared the results obtained this way, with those from a commercial finite-element code (ANSYS 7.0) based on the formulation $A - V$ [1], again with respect to the *same* mesh of 30782 tetrahedra. In Table I we show the amplitude of the voltage variation ΔU instead of ΔZ when $\Delta \mathrm{x} = 7.5$ mm. We used the same iterative solver for nonsymmetric sparse complex matrices in the three cases based on a conjugate gradient squared iterative method with SSOR preconditioning (the over-relaxation coefficient used is $\omega = 1.7$) of the NAG scientific library; the CPU time on a portable Pentium IV with 0.5 GB RAM, 1.9 GHz is about the same in the three cases (88 s as maximum, of which, 68 s for generating geometric data and assembling the final system, while 20 s are needed for its solution, in 87 iterations) for one eddy-current analysis.

Finally, in Fig. 4, we compare the convergence of Z_d (on the top) and ΔU (on the bottom), when the number of elements is increased up to 130 000 (14.50 min of CPU time, 140 iterations). With ANSYS, we avoided simulations above 40 000 elements due to heavy memory requirements.

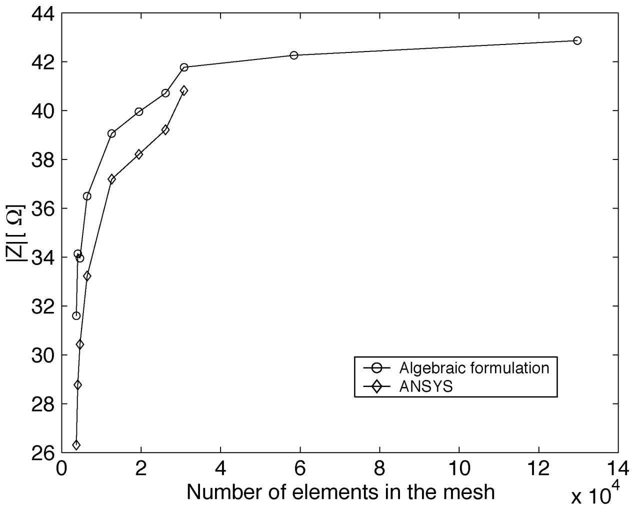

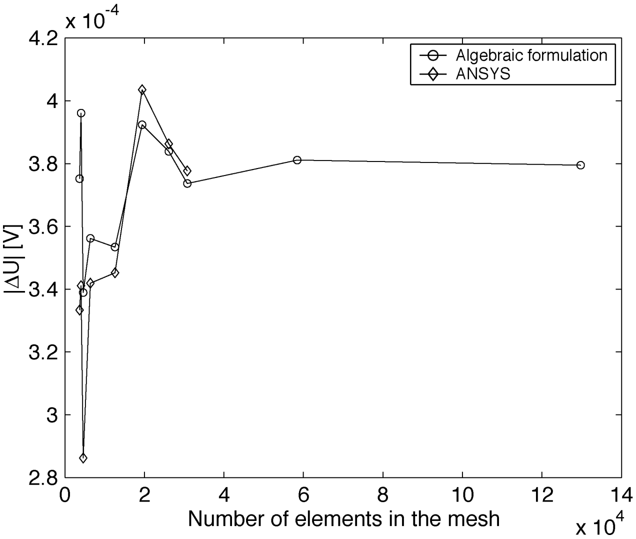

Fig. 4. Covergence of $|Z_d|$ (on the top) and of $|\Delta U|$ (on the bottom) values versus the number of tetrahedra.

VII. Conclusion

The geometric frame of Tonti's diagram is used to derive the algebraic equations of the so-called A-χ geometric formulation for 3-D eddy currents. Different approaches to construct magnetic and Ohm's discrete constitutive matrices have also been proposed evidencing how to construct a symmetric Ohm's matrix. Finally, we suggested a way to compute the current sources consistently with discrete continuity law, so that an ungauged approach can be efficiently applied. The results, thus obtained, are in a very good agreement with those from a commercial FE code.

Acknowledgment

The authors would like to thank Prof. E. Tonti for his helpful suggestions about the diagrams.

References

[1] O. Biro and K. Preis, "On the use of the magnetic vector potential in the finite element analysis of three-dimensional eddy currents," *IEEE Trans. Magn.*, vol. 25, no. 4, pp. 3145–3159, Jul. 1989.

[2] O. Biro, K. Preis, G. Vrisk, K. R. Richter, and I. Ticar, "Computation of 3-D magnetostatic fields using a reduced scalar potential," *IEEE Trans. Magn.*, vol. 29, no. 2, pp. 1329–1332, Mar. 1993.

[3] A. Bossavit, "The crack as a symmetry-breaker, and implications," a contribution to the "MANODET" project, May 1999.

[4] ——, "A rationale for edge-elements in 3-D fields computations," *IEEE Trans. Magn.*, vol. 24, no. 1, pp. 74–79, Jan. 1988.

[5] ——, *Computational Electromagnetism*. New York: Academic, 1998.

[6] A. Bossavit, "How weak is the weak solution in finite elements methods," *IEEE Trans. Magn.*, vol. 34, no. 5, pp. 2429–2432, Sep. 1998.

[7] A. Bossavit and L. Kettunen, "Yee-like schemes on staggered cellular grids: A synthesis between FIT and FEM approaches," *IEEE Trans. Magn.*, vol. 36, no. 4, pp. 861–867, Jul. 2000.

[8] P. Bettini, E. Cardelli, M. Cioffi, P. Di Barba, A. Faba, F. Ferraioli, A. Formisano, R. Martone, F. C. Morabito, M. Morozov, G. Rubinacci, A. Savini, R. Specogna, A. Stella, A. Tamburrino, F. Trevisan, S. Ventre, M. Versaci, and F. Villone, "Direct and inverse electromagnetic methodologies: the proposal of MADEND project for ECT analysis," in *Proc. PIERS 2004*, Pisa, Italy, Mar. 28–31, pp. 731–734.

[9] L. Codecasa, V. Minerva, and M. Politi, "Use of barycentric dual grids for the solution of frequency domain problems by FIT," *IEEE Trans. Magn.*, vol. 40, no. 2, pp. 1414–1419, Mar. 2004.

[10] M. Cinalli, F. Edelvik, R. Schuhmann, and T. Weiland, "Consistent material operators for tetrahedral grids based on geometrical principles," *Int. J. Numer. Model.*, vol. 17, pp. 487–507, 2004.

[11] H. Flanders, *Differential Forms With Applications to the Physical Sciences*. New York: Academic, 1963.

[12] Y. Le Menach, S. Clenet, and F. Piriou, "Determination and utilization of the source field in 3D magnetostatic problems," *IEEE Trans. Magn.*, vol. 34, no. 5, pp. 2509–2512, Sep. 1998.

[13] MADEND project web site. [Online]. Available: http://143.225.250.2/dii/Madend/

[14] H. Igarashi and T. Honma, "On convergence of ICCG applied to finite-element equation for quasistatic fields," *IEEE Trans. Magn.*, vol. 38, no. 2, pp. 565–568, Mar. 2002.

[15] B. Weiss and O. Biro, "On the convergence of transient eddy-current problems," *IEEE Trans. Magn.*, vol. 40, no. 2, pp. 957–960, Mar. 2004.

[16] S. Reitzinger and M. Kaltenbacher, "Algebraic multigrid methods for magnetostatic field problems," *IEEE Trans. Magn.*, vol. 38, no. 2, pp. 477–480, Mar. 2002.

[17] M. Marrone, "A new consistent way to build symmetric constitutive matrices on general 2D grids," *IEEE Trans. Magn.*, vol. 40, no. 2, pp. 1420–1423, Mar. 2004.

[18] T. Tarhasaari, L. Kettunen, and A. Bossavit, "Some realizations of a discrete Hodge operator: A reinterpretation of finite elements techniques," *IEEE Trans. Magn.*, vol. 55, no. 3, pp. 1494–1497, May 1999.

[19] E. Tonti, "On the formal structure of physical theories," Quaderni dei Gruppi di Ricerca Matematica del CNR, 1975.

[20] ——, "Algebraic topology and computational electromagnetism," in *Proc. 4th Int. Workshop on Electric and Magnetic Fields*, Marseille, France, May 12–15, 1988, pp. 284–294.

[21] ——, "On the geometrical structure of electromagnetism," in *Gravitation, Electromagnetism and Geometrical Structures for the 80th Birthday of A. Lichnerowicz*, G. Ferrarese, Ed. Bologna, Italy: Pitagora Editrice, 1995, pp. 281–308.

[22] ——, "Finite formulation of the electromagnetic field," *IEEE Trans. Magn.*, vol. 38, no. 2, pp. 333–336, Mar. 2002.

[23] F. Trevisan and L. Kettunen, "Geometric interpretation of discrete approaches to solving magnetostatics," *IEEE Trans. Magn.*, vol. 40, no. 2, pp. 361–365, Mar. 2004.

[24] F. Trevisan, "3-D eddy current analysis with the cell method for NDE problems," *IEEE Trans. Magn.*, vol. 40, no. 2, pp. 1314–1317, Mar. 2004.

Manuscript received November 7, 2004; revised January 26, 2005.